INDUCTICA TECHNICAL CONFERENCE Berlin 2012

Conference Proceedings

C W I E M E Berlin 2012

Coil Winding, Insulations & Electrical Manufacturing International Conference and Exhibition

26, 27, 28 June 2012

Messe Berlin, Berlin, Germany

Coil Winding, Insulation & Electrical Manufacturing Exhibitions

U.K. Office: PO Box 7683,
Sturminster Newton, Dorset DT10 9BF, UK
Tel: +44(0)1258 446280 Fax: +44(0)1258 446355
E-mail: cwiemeuk@coilwindingexpo.com

U.S.A. Office: 28W117 Countryview Drive,
Naperville, IL 60564
Tel: 630-355-0955 Fax: 630-355-0956
E-mail: cwiemeusa@coilwindingexpo.com

www.coilwindingexpo.com

Iron-loss model for the FE-simulation of electrical machines

Simon Steentjes, Daniel Eggers, Marc Leßmann and Kay Hameyer
Institute of Electrical Machines (IEM), RWTH Aachen University, 52062 Aachen, Germany

The accurate prediction of iron losses of soft magnetic materials for various frequencies and magnetic flux densities is eminent for an optimal design of electrical machines. For this purpose different phenomenological iron-loss models have been proposed describing the loss generating effects. Most of these suffer from poor accuracy for high frequencies as well as high values of magnetic flux densities. This paper presents an approach for advanced iron-loss computation. The proposed IEM-Formula resolves the limitation of the common iron-loss models by introducing a high order term of the magnetic flux density. Exemplary, the iron-loss formula is utilized to calculate the iron losses of an induction machine for the drive train of a full electric vehicle.

I. Introduction

For the development and electromagnetic design of high efficiency electrical machines there is a strong need for improved and more accurate iron-loss models. Due to the increasing motor speed, respectively supply frequency of the machines, a wide operational range of frequency f and magnetic flux density B – in particular for the electrical machines with elevated operating frequencies such as the ones incorporated into hybrid or full-electric drive trains of vehicles – is required. The inverter supply with pulse-width modulation additionally induces higher harmonics into the machine causing further losses, which have to be considered. Such improved iron-loss estimation for losses occurring in the machine's stator and rotor parts is indispensable in order to effectively carry out electromagnetic and thermal design. Accurate loss calculation forms the basis for the selection of the most appropriate electrical steel grade which suits best the specific working conditions in the rotating electrical machine.

This paper presents a modified iron-loss model that is derived from the well-known classical Bertotti formulation [Bertotti, 1998]. Purpose is to better suit the experimentally observed iron-loss characteristics at high magnetic flux density levels by including a term depending on a power of magnetic flux density B which is higher than two (B^2 is the power of the Foucault losses [Lammeraner, 1967]). This model is extended to further consider rotational losses and higher harmonics. For verification a comparison of this model with unidirectional standard and non-standard measurements is performed and an example of use is given.

II. Iron-loss modeling

According to the well-known loss separation principle [Bertotti, 1998], the iron losses in electrical steel laminations can be split up into three parts:

a) the Foucault eddy current losses, calculated in a classical, macroscopic way with Maxwell's equations [Bertotti, 1998][Lammeraner, 1967],
b) the hysteresis losses, and
c) the excess losses, associated with the presence of domains, leading to various space-time dependencies in the magnetization process [Bertotti, 1998].

In general, the iron losses in soft magnetic materials are measured and theoretically estimated under specific, standardized conditions such as the Epstein test under uniaxial and purely sinusoidal magnetic flux density. However, magnetic flux paths occurring in rotating electrical machines are more complex than in the case of material characterization of the Epstein-strips. Thus, the actual iron losses occurring in electrical machines cannot be placed in a simple relationship to the Epstein loss data. In addition, these approaches are insufficient if new machine designs with higher material utilization are introduced (higher peak values of the magnetic flux density B) and higher operating frequencies f are attained.

Additional reasons for this lack of accuracy could be summarized as follows:

- harmonics of the magnetic flux waveform due to iron saturation, skin effect, stator slots, and supply / load currents (e.g. pulse-width modulation),
- the rotating electrical machine has important differences compared to the standardized conditions of the Epstein-test such as geometry and non-unidirectional magnetization conditions, resulting in rotational losses,
- changes in the magnetic properties of the material during the production process due to residual stresses and applied stresses such as cutting effects.

Therefore, these parasitic effects should be considered and included in the iron loss calculation to more accurately predict the iron losses. Up to a certain degree this is aimed in the proposed improved iron loss model.

III. Extension of common iron-loss models

Epstein measurements are performed under uniaxial (in space) and sinusoidal (in time) magnetic flux density. Thus, magnetic flux density in Epstein frame measurements is completely represented by its fundamental wave. However, in rotating electrical machines this is not the case: higher harmonics (in time) due to iron saturation, skin effect, stator yoke slots and the use of a power electronics supply (inverter, PWM) can occur, as well as vector magnetic fields (in space), the latter giving rise to so-called rotational losses.

In order to improve common iron-loss models to these conditions, rotational losses and higher harmonics have to be considered by [Bertotti et al, 1994] [Fiorillo et al, 1993] [Fiorillo et al, 1990a] [Fiorillo et al, 1990b]:

1. A Fourier analysis of the magnetic flux density waveform during one electrical period to identify the higher harmonics;
2. The level of magnetic flux distortion and also the (technical) saturation. Two parameters B_{min} and B_{max}, respectively the minimal and maximal magnetic flux density amplitudes over one electrical period, serve for this. The locus of the magnetic flux density vector over one electrical period is characterized by B_{min} and B_{max}. This enables to identify the level of magnetic flux distortion by taking the ratio between B_{min} and B_{max}. B_{max} gives an idea about the level of saturation. Zones within the stator with rotational hysteresis are those with large values of B_{min}, whereas unidirectional field corresponds with a zero value of amplitude B_{min}.

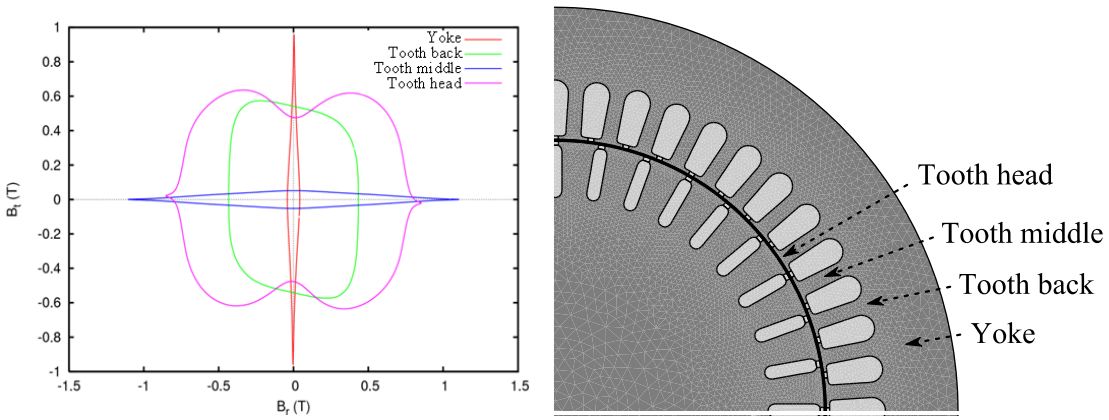

Figure 1: *Flux distortion (described in tangential(B_t) and radial (B_r) coordinates) at different points of the machine as indicated on the right.*

In the accentuated loci (Figure 1) of the stator laminations, the different magnetizations types can be found. The diagram of Figure 1 indicates that there are unidirectional magnetizations in the middle of the teeth, whereas elliptical up to nearly circular magnetizations can be found at the back and head of teeth.

IV. IEM-Formula

The IEM proposes and validates an additional loss term P_{sat} with a higher order of B dependence:

$$P_{IEM}(B,f) = P_{hyst}(B,f) + P_{classic}(B,f) + P_{excess}(B,f) + P_{sat}(B,f) \quad \{1\}$$

with the following loss contributions:

$$P_{hyst}(B,f) = a_1 \cdot \left(1 + \frac{B_{min}}{B_{max}} \cdot \left(r_{hyst}(B_{max}) - 1\right)\right) \cdot B_{max}^2 \cdot f, \quad \{2\}$$

$$P_{classic}(B,f) = a_2 \cdot \sum_{n=1}^{\infty}(B_{n,x}^2 + B_{n,y}^2) \cdot (nf)^2, \quad \{3\}$$

$$P_{excess}(B,f) = a_5 \cdot \left(1 + \frac{B_{min}}{B_{max}} \cdot (r_{excess}(B_{max}) - 1)\right) \cdot \sum_{n=1}^{\infty}\left(B_{n,x}^{1.5} + B_{n,y}^{1.5}\right) \cdot f^{1.5}, \quad \{4\}$$

$$P_{sat}(B,f) = a_2 \cdot a_3 \cdot B_{max}^{a_4+2} \cdot f^2. \quad \{5\}$$

For that, B_{max} is the amplitude of the fundamental frequency component of the flux density in Tesla [T], B_n the amplitude of the n-th harmonic component of the magnetic flux density in Tesla [T], n the order of harmonic, f the fundamental frequency in Hertz [Hz], $a_1 - a_5$ the material specific parameters and r_{hyst}, r_{excess} the rotational loss factors.

The *IEM-Formula* is based on adding analytical descriptions to include the mentioned additional effects:

- The eddy current and excess loss description of the classical Bertotti formula [Bertotti, 1998] is extended with a summation over all harmonics [Fiorillo et al, 1990a, b] in order to take the influences of harmonics into account.
- Subsequently the hysteresis and excess loss terms are extended to model the influence of rotational and flux distortion effects on the corresponding losses [Bertotti et al, 1994] [Fiorillo et al, 1993].
- Finally the influence of the nonlinear magnetization behavior at higher magnetic flux densities is included using an additional higher order term in B $\{5\}$.

V. Comparison to standardized measurements

The parameters $a_1 - a_5$ used in $\{2 - 5\}$ are identified on the one hand by a pure mathematical fitting procedure performed on the measured data sets and on the other hand by a semi-physical identification procedure.

For the semi-physically parameter identification, the parameter a_1 for the hysteresis loss component is identified by mathematical fitting of dc measurements (quasi-static measurements) at a standard Epstein frame with 700 windings and 12 strips of the soft magnetic material, each 280mm x 30mm, at sinusoidal uniaxial magnetic flux densities. The parameter a_2 for the classical eddy current losses is calculated by the equation

$$a_2 = \frac{\pi^2 d^2}{6\rho\rho_e} \quad \{6\}$$

with the sheet thickness d, the material specific density ρ and the specific electrical resistivity ρ_e of the soft magnetic material. The excess loss parameter a_5 is identified by measurements at the Epstein frame with 700 windings at low frequencies between $5Hz$ and $10Hz$. In this frequency range the eddy current losses are negligible and the excess loss term is easily separated. The

parameters a_3 and a_4 are determined from the iron-loss estimation error

$$P_{error} = P_{measured} - (P_{hyst} + P_{classic} + P_{excess}) . \quad \{7\}$$

The measurements for the identification of the parameters are performed in a frequency range from $500Hz$ to $2000Hz$ on two Epstein frames with 100 and 40 windings for sinusoidal uniaxial magnetic flux densities. The Epstein frame with 100 windings is used for frequencies from $500Hz$ up to $1500Hz$ and the frame with 40 windings from $1500Hz$ upwards.
Here, the non-oriented electrical steel grade M270-35A is studied. Table I presents the resulting parameters obtained by the mathematical fitting and semi-physical identification.

	a_1	a_2	a_3	a_4	a_5
Mathematical	$9.89 \cdot 10^{-3}$	$26.39 \cdot 10^{-6}$	0.19	5.15	$0.89 \cdot 10^{-3}$
Semi-Physical	$11.70 \cdot 10^{-3}$	$50.34 \cdot 10^{-6}$	0.1	4.30	$0.45 \cdot 10^{-3}$

Table I: Mathematical and semi-physical identified parameter sets of the IEM loss model {1}.

Using these parameters the predicted iron losses by the *IEM-Formula* {1} are compared to measurements at an Epstein frame under uniaxial sinusoidal magnetic flux densities. The results for two exemplary frequencies are shown in Figure 2.

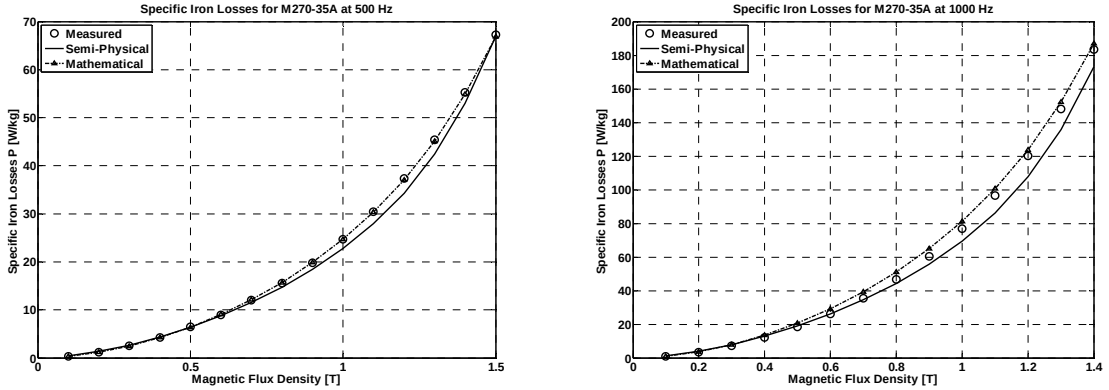

Figure 2: *Comparison of the IEM-Formula {1} with measurements for M270-35A at a frequency of 500 Hz (left) and 1000Hz (right) using the parameters of Table I.*

The IEM-Formula describes the loss behavior accurately using the high order term in B {5}. The mathematical parameters yield more accurate loss prediction. The average relative error of both parameter sets is below 10%.

VI. Comparison to non-standard measurements

The *IEM-Formula* is compared to non-standard measurements, i.e. measurements with harmonic contents imposed in the magnetic flux density waveform. The used parameter set consists of the one identified under sinusoidal uniaxial magnetic flux density conditions. The Epstein measurement results in an experimental iron-loss value corresponding with the non-sinusoidal magnetic flux density waveform. On the other hand, the IEM loss model {1} is applied to these conditions by the given values for the harmonics' frequencies and the amplitudes, giving rise to a calculated iron-loss value, which then can be benchmarked against the experimental value. With this method the accuracy and reasonability of the model extensions for higher harmonics and the additional effects in the *IEM-Formula* are studied in detail. Calculated iron losses are compared with measurements at 400Hz fundamental frequency and two different magnetic flux density amplitudes with harmonics of the order 5 and 9 (Figure 3, 4).

The presented resulting losses for different flux density waveforms, calculated as well as measured, emphasize the accuracy of the developed loss model. The accuracy is increasing for ascend flux density amplitudes. The model predicts the iron losses in the saturation region with a deviation of less than 2%, in the linear region of the single-valued curve the deviation is less than 4%. Furthermore the model predicts the loss values with the same accuracy for different amounts of harmonics. Although it is a rather mathematical model, the results obtained serve as a first validation of the higher harmonic term in the *IEM-Formula*.

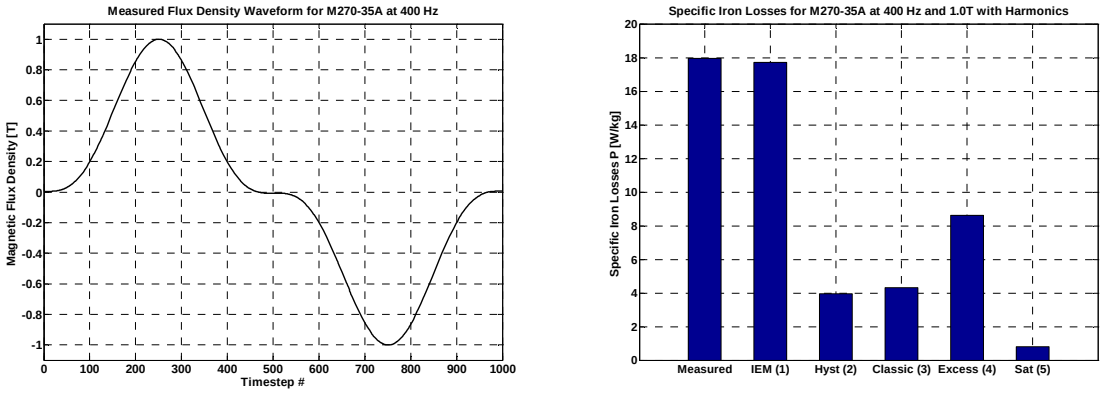

Figure 3: *Comparison of the IEM-Formula {1} with non-standard measurements at a fundamental frequency of 400 Hz and magnetic flux density of 0.78T (right). On the left the used magnetic flux density waveform is shown.*

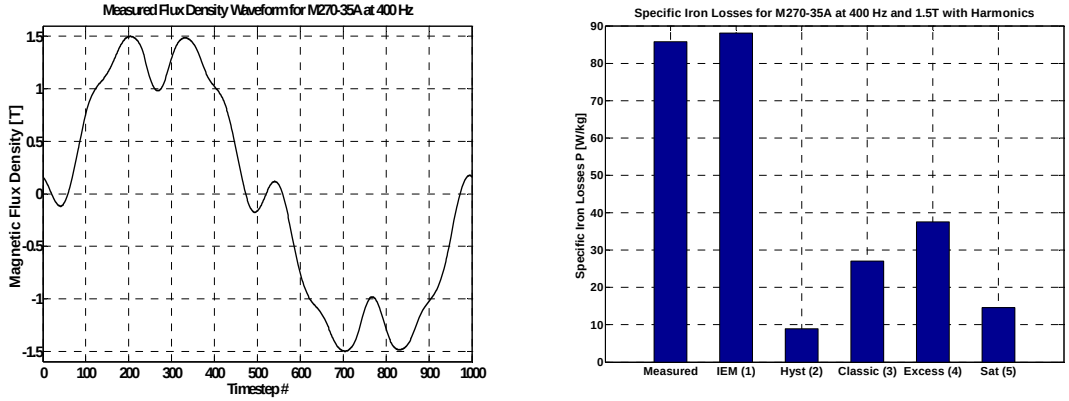

Figure 4: *Comparison of the IEM-Formula {1} with non-standard measurements at a fundamental frequency of 400 Hz and magnetic flux density of 1.5T (right). On the left the used magnetic flux density waveform is shown.*

VII. Induction machine loss analysis

i. Induction machine model

The *IEM-Formula* is exemplarily employed to an induction machine model. Single-valued magnetization curves have been used to consider saturation effects originating from the non-linear material behavior. Second-order effects, originating from hysteresis behavior, are neglected. Pure hysteresis, classical and excess losses in the laminated stator and rotor cores are estimated a posteriori using the local waveforms of the magnetic flux densities in {1}.

The cross section of the laminated stator and rotor core of the 8 pole induction machine under consideration is shown in Figure 1. To reduce the 5^{th} and 7^{th} harmonic, a distributed and chorded winding with 5/6 pitch is used. Transient 2-D computations of the field distribution have been

performed by in-house FE-solver iMOOSE [IEM, 2012]. The magnetic flux density distribution for one simulation step at nominal operation is shown in Figure 5.

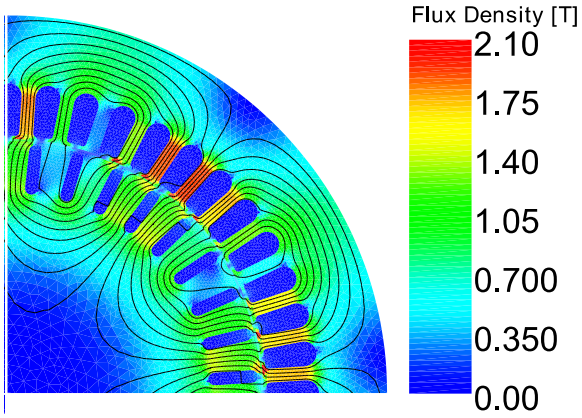

Figure 5: *Magnetic flux density distribution at one simulation step.*

ii. Iron losses in stator & rotor

The iron losses of the studied induction machine are calculated in the post process of the FE-simulation by adapting the *IEM-Formula* {1} on one electrical period, Figure 6 - 8.

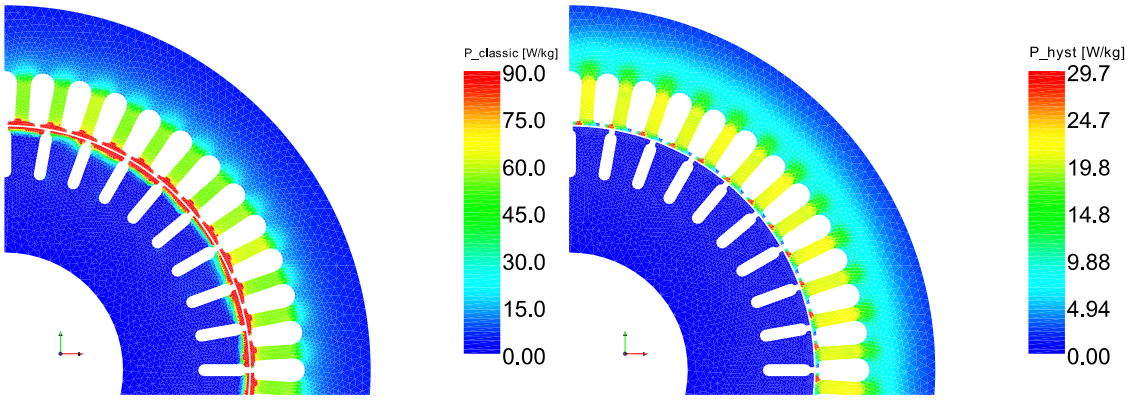

Figure 6: Illustration of the classical loss (left) and hysteresis loss (right) distribution of the investigated induction machine for iron-loss calculation with {1}.

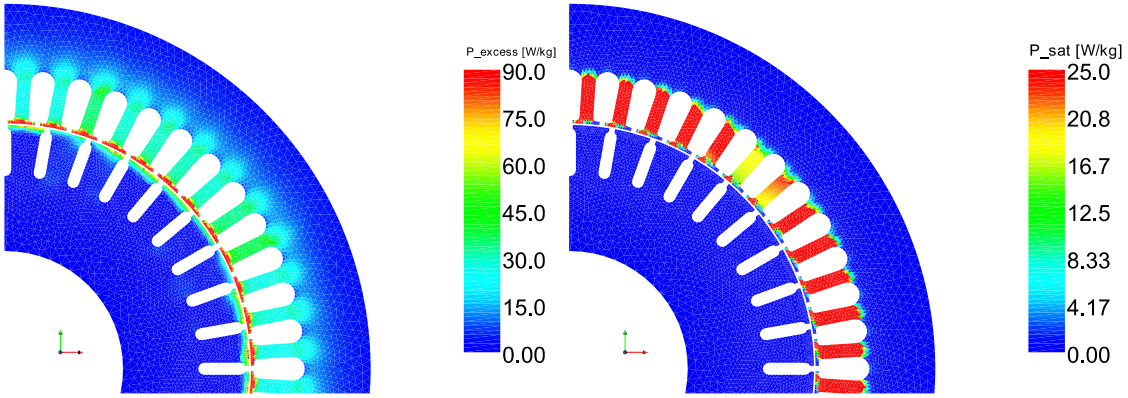

Figure 7: Illustration of the excess loss (left) and saturation loss (right) distribution of the investigated induction machine for iron-loss calculation with {1}.

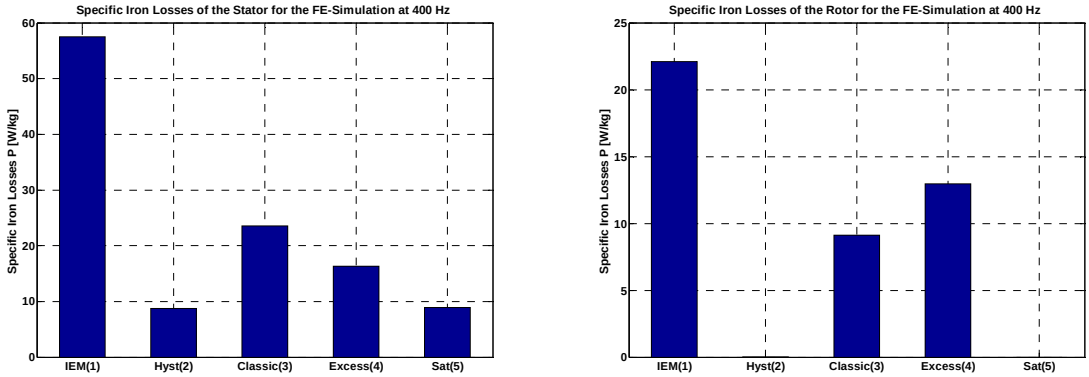

Figure 8: *Visualization of the loss contributions of stator and rotor of the investigated induction machine for iron loss calculation with {1}.*

iii. B_{min} and B_{max} distribution

In order to determine the level of saturation and magnetic flux distortion, the figures of B_{max} and B_{min} (Figure 9). B_{max} and B_{min} are the extremum amplitudes of B, evaluated over a complete period, at each mesh element.

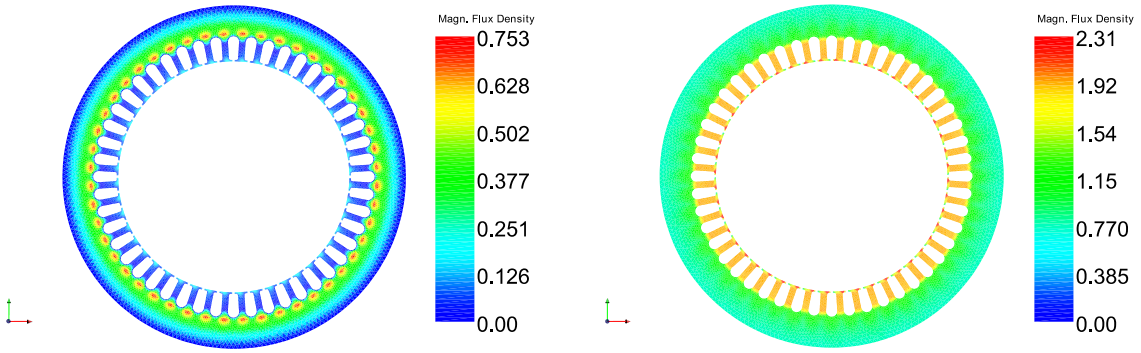

Figure 9*: B_{min} (left) and B_{max} (right) distribution.*

iv. Discussion

The numerical simulation of induction reveals the following physical phenomena: 1) Magnetic saturation in the tooth middle and head, 2) significant rotational flux in the back of tooth, 3) high harmonic pulsations in the local flux waveforms due to stator and rotor slots as well as saturation effects. As shown in Figure 6 and 7, the main contribution to each fraction of total specific losses occurs in the magnetically high exploited stator teeth at nominal rotor speed of $n = 5925\, min^{-1}$. The ratio B_{min}/B_{max}, indicating rotational flux, is identified by observing the amount of minimal and maximal flux density for each finite element of the yoke for one electrical period. Areas of high rotational flux can be found in the back of tooth, inducing increased rotational hysteresis losses in these regions of yoke (Figure 6 and 9).

A Fast-Fourier-Analysis observes a significant impact of the 7^{th} and 9^{th} harmonic, which increase the classical losses compared to the fundamental by approximately 28%. The excess and saturation losses mainly occur in regions of high flux densities (head of stator and rotor tooth, middle of stator tooth), whereas an additional appearance of excess losses can be found in the back of stator teeth. Due to the comparatively low rotor flux density and frequency of fundamental, the rotor losses are mainly limited to the rotor teeth, induced by harmonics of stator and rotor slots.

V. Conclusions

This paper presents a modified iron-loss model for the accurate iron-loss estimation under non ideal magnetization conditions. The model considers harmonics as well as rotational magnetization and

saturation effects. The accuracy of the computed iron losses for harmonics under saturation is shown by the comparison of simulations to measurements under non-sinusoidal excitations at an Epstein frame. The model of an induction machine is taken as an example to calculate the iron losses. Additional studies regarding the influence of minor loops and the rotational loss behavior will be conducted in the next steps of this research work.

References

[Bertotti, 1994] G. Bertotti, A. Canove, M. Chiampi, D. Chiarabaglio, F. Fiorillo, A.M. Rietto, "Core loss prediction combining physical models with numerical field analysis," *J. Magn. Magn. Mat.*, vol. 133, pp. 647-650, 1994.

[Bertotti, 1998] G. Bertotti, *Hysteresis in Magnetism: For Physicists, Materials Scientists, and Engineers*, Academic Press, 1998.

[Fiorillo et al, 1990a] F. Fiorillo and A. Novikov, "An Improved Approach to Power Losses in Magnetic Laminations under Nonsinusoidal Induction," *IEEE Trans. Magn.*, vol 26, no. 5, 1990.

[Fiorillo et al, 1990b] F. Fiorillo and A. Novikov, "Power losses under sinusoidal, trapezoidal and distorted induction waveform," *IEEE Trans. Magn.*, vol. 26, no. 5, pp. 2559 - 2561, 1990.

[Fiorillo et al, 1993] F. Fiorillo and A. M. Rietto, "Rotational versus alternating hysteresis losses in nonoriented soft magnetic laminations," *J. Appl. Phys.*, vol. 73, pp. 6615-6617, 1993.

[IEM, 2012] Institute of Electrical Machines, www.iem.rwth-aachen.de, 15.05.2012.

[Lammeraner, 1967] J. Lammeraner and M. Stafl, *Eddy Currents*, Iliffe, 1967.